Journal of Applied Polymer Science

Effects of molecular weight and grafted maleic anhydride of functionalized polylactic acid used in reactive compatibilized binary and ternary blends of polylactic acid and thermoplastic cassava starch

Sukeewan Detyothin,[1,2] Susan E. M. Selke,[1] Ramani Narayan,[3] Maria Rubino,[1] Rafael A. Auras[1]

[1]School of Packaging, Michigan State University, East Lansing, Michigan 48824

[2]Department of Agro-industry, Naresuan University, Phitsanulok 65000, Thailand

[3]Department of Chemical Engineering and Materials Science, Michigan State University, East Lansing Michigan 48824

Correspondence to: R. A. Auras (E-mail: aurasraf@msu.edu)

ABSTRACT: Polylactic acid (PLA) was reactively functionalized with maleic anhydride (MA) and 2,5-bis(*tert*-butylperoxy)−2,5-dimethylhexane (Luperox 101 or L101) using a twin screw extruder (TSE). The effects of functionality (grafted MA level) and/or number average molecular weight of functionalized PLA (PLA-*g*-MA) as the reactive polymer pairs (binary blends) and reactive compatibilizer (ternary blends) were investigated. Due to the dominant side reaction during melt free radical grafting, polymer degradation or chain scission, PLA-*g*-MA having a higher grafted MA had lower molecular weights and intrinsic viscosity as well as broader molecular weight distribution values. The thermal, physical, mechanical, and morphological properties of binary blends produced by using the TSE and injection molding at a ratio of 70 wt % PLA-*g*-MA and 30 wt % thermoplastic cassava starch (TPCS) were analyzed. The reactive blends having grafted MA more than 0.4 wt % had poor tensile strength and elongation at break. Similar trends in morphology and tensile properties were observed in the reactive ternary blends. The use of PLA-g-MA strongly impacted the elongation at break but not the modulus or tensile strength. An increase of PLA-*g*-MA's number average molecular weight ($\overline{M}_n$ or M_n) improved the tensile properties of the blends. The reactive ternary blend having 0.1 wt % grafted MA on PLA and PLA-*g*-MA basis and PLA-*g*-MA's M_n of 45 kDa offered the highest elongation at break. © 2015 Wiley Periodicals, Inc. J. Appl. Polym. Sci. **2015**, *132*, 42230.

KEYWORDS: biodegradable; biopolymers and renewable polymers; polyesters; polysaccharides; synthesis and processing

Received 13 November 2014; accepted 17 March 2015

DOI: 10.1002/app.42230

INTRODUCTION

Polylactic acid (PLA), a biobased, recyclable, and biodegradable polymer, is mostly used to replace commercial petroleum-based polyesters when environmental issues are a concern. PLA is a stiff and brittle material with mechanical properties comparable to polystyrene (PS) and is widely used in textiles, packaging, medical, and automotive applications.[1] However, some PLA properties such as low elongation at break, poor flexibility and toughness, low heat deflection temperature (HDT), and slow nucleation and crystallization limit its commercial uses.[2] Blending of PLA with other polymers is one of the most cost-effective methodologies to tailor-make the desired properties of the blend. Blends of PLA with non-biodegradable polymers (e.g., polyolefins, vinyl and vinylidene chloride, elastomers, and rubbers), biodegradable polymers (e.g., polyanhydrides, aliphatic polyesters, aliphatic-aromatic copolyesters, lipids, proteins, and carbohydrates), and plasticizers have been extensively reported.[3,4]

Starch is one of the best candidate polymer pairs to blend with PLA whenever cost, renewable resources, and biodegradability are considered. Starch acts as a nucleating agent, enhancing the crystallization rate of PLA.[4] Furthermore, the use of thermoplastic starch (TPS) imparts flexibility and ductility to PLA. However, PLA, a hydrophobic material, and starch, a hydrophilic material, have different chemical structures, resulting in different surface energies and incompatibility. Physical blending of TPS and PLA produces immiscible blends.[5,6]

Reactive compatibilization is an effective tool to improve compatibility of polymer pairs.[7] The first step, functionalization, generates reactive polymers by mixing of functional groups (e.g., anhydride, isocyanate, and epoxide), suitable initiators (e.g., peroxide), and non-reactive polymers. The next step, reactive blending, occurs when the reactive polymer forms a graft copolymer with the polymer pair directly at the interface. As a consequence, interfacial tension of the two immiscible phases is decreased, and interfacial adhesion improves, resulting in a finer

and more uniform/stable morphology as well as facilitating stress (energy) transfer between the two phases, improving their mechanical properties.[8] Among the functional groups, maleic anhydride (MA), a polar monomer, is preferably used due to its low toxicity, high reactivity, low potential to polymerize itself under free radical grafting conditions, and ease of handling.[9,10]

The use of grafted MA for reactive compatibilization of starch and biodegradable polymers is extensively reviewed elsewhere; some of this work showed the effects of grafted MA levels (amounts) on properties of starch and other polymers (e.g., PLA, poly(butylene-adipate-co-terephthalate) (PBAT), poly(ε-caprolactone) (PCL), polypropylene (PP), and polyethylene (PE)). In all these works, the grafted MA levels are usually referred as nominal content or amount of MA and peroxides rather than measured grafted MA content.[9–15] However, the effect of molecular weight of the functionalized polymers on the properties of starch and other polymers has scarcely been investigated. Improvement in properties due to use of functionalized polymers having higher molecular weight has been reported to involve, i.e., finer and more stable morphology of polystyrene/PS grafted MA/polyamide 6 (PA 6), and an increase of storage moduli of maleinized soybean oil triglycerides/epoxidized soybean oil triglycerides/PP grafted MA blends.[16,17]

In this work, PLA-*g*-MA having different amounts of grafted MA and/or M_n was generated using a twin-screw extruder (TSE). PLA-*g*-MA properties were examined. This work uniquely assessed the effects of grafted MA level and molecular weight on the properties and morphology of the reactive binary and ternary blends with thermoplastic cassava starch (TPCS) and PLA. Novel TPCS and PLA binary and ternary blends were produced for industrial applications such as packaging and agriculture films.

MATERIALS AND METHODS

Materials

Ingeo™ Biopolymer 2003D poly(96% L-lactic acid), (PLA), was provided by NatureWorks LLC (Minnetonka, MN). Tapioca starch (cassava starch) was donated by Erawan Marketing (Bangkok, Thailand). Food grade glycerol (>99%), MA (95%), and L101 (90%) were obtained from Sigma-Aldrich Chemical Company (Milwaukee, WI). All materials and chemical agents were used as received or as later specified.

Compounding of TPCS

Cassava starch was premixed with glycerol at a ratio of 70/30 by weight and kept for around 12 h before compounding in a co-rotating TSE CENTURY ZSK-30 (Traverse City, MI), having a screw diameter of 30 mm and a length/diameter (L/D) ratio of 42/1. Compounding of TPCS was performed at a temperature profile from the feed throat to the die of 25/100/105/110/115/120/120/120/115/115°C and a screw speed of 125 rpm. The extruded strands were blown air cooled and kept in an aluminum container at 23 ± 2°C and 50 ± 10% relative humidity (RH).

Reactive Functionalization of PLA and Determination of Grafted MA on PLA

PLA resin, dried in a vacuum oven at 90°C for 6 h, was premixed with ground MA and L101. The reactive functionalization of PLA (to produce PLA-*g*-MA) took place in a 32-mm counter-rotating conical TSE (C.W. Brabender Instruments South Hackensack, NJ) with a L/D ratio of 13/1 at a temperature profile from the feed throat to the die of 165/185/185/165°C. The compositions and screw speeds used are listed in Table I. MA and L101 concentrations and TSE screw speed were determined from preliminary work conducted by the authors.[6] The weight percentages of MA and L101 used were based on PLA weight. The processing temperatures and screw speeds of TSE were set to get complete decomposition of L101 ($t_{1/2}$ = 69 s @ 180°C) with no residual and minimize thermal degradation of PLA.[18] After reactive functionalization, the extruded strands were cooled by blown air, pelletized, and kept in an aluminum container at 23 ± 2°C and 50 ± 10% RH.

Table I. Sample Composition and Screw Speed for Production of PLA-*g*-MA

Sample	Nominal MA (wt %)	L101 (wt %)	TSE screw speed (Rpm)
PLA-*g*-MA A	4.5	0.047	18
PLA-*g*-MA B	2	0.2	10
PLA-*g*-MA C	4.5	0.425	18
PLA-*g*-MA D	2	0.65	10
PLA-*g*-MA E	2	0.65	25
PLA-*g*-MA F	7	0.65	10

To determine the percentage grafting, the PLA-*g*-MA resins were vacuum dried at 130°C for 24 h to remove unreacted MA, purified and hydrolyzed to convert the anhydride groups into carboxylic acid groups, and then titrated. Details of this modified methodology are described elsewhere.[19]

Reactive Blending of Binary and Ternary Polymers

For producing the binary polymer blends, PLA or PLA-*g*-MA resins were blended with TPCS resins at a ratio of 70/30 by weight. Before blending, PLA, PLA-*g*-MA, and TPCS resins were dried under vacuum at 90°C for 6 h, 130°C for 24 h, and air-dried at 60°C for two days, respectively. The dried resins were premixed and then fed into a vertical mini co-rotating TSE (DSM Micro 15 compounder, DSM, The Netherlands), having a screw length of 150 mm, an L/D ratio of 18, and a net capacity of 15 cc. The molten extrudates were shaped into disk, bar, and dumbbell specimens using a mini injection molder (TS/-02 DSM), having maximum injection pressure of 150 psi. The extrusion and injection conditions are listed in Table II, with the conditions for PLA resins provided for comparison. Detailed information about how the conditions were derived is provided elsewhere.[6] Sample 7PT, a non-reactive or physical blend, was a blend of PLA and TPCS, while samples 7rPT A, B, C, and D identified the reactive blends, the blends produced with TPCS and PLA-*g*-MA A, B, C, and D, respectively. Binary polymer blends were stored at 23°C and 0% RH until testing.

The ternary polymer blends were also produced in the DSM Micro 15 compounder. Dried PLA, PLA-*g*-MA, and TPCS resins were weighed and mixed at various ratios (Table III). The extrusion and injection conditions are shown in Table III. The MA content in the reactive blends is weight of MA based on PLA

Table II. Extrusion and Injection Molding Conditions of PLA, Physical Blend (7PT), and Reactive Binary Blends (7rPT A, B, C, and D)

Sample	Extrusion condition: temperature profile (°C), screw speed (rpm), and residence time (min)	Injection molding condition: temperatures of transfer tube/mold (°C), mold residence time (s), injection pressure (psi)
PLA	190/190/190, 100, 5	190/38, 10, 145
7PT	172/172/172, 100, 5	173/38, 10, 150
7rPT A	167/167/167, 100, 5	168/38, 10, 140
7rPT B	167/167/167, 100, 5	168/38, 10, 120
7rPT C	160/160/160, 100, 5	162/38, 10, 140
7rPT D	160/160/160, 100, 5	162/38, 10, 100

and PLA-*g*-MA.[6] Ternary polymer blends were stored at 23°C and 0% RH. Blends were tested not later than 1 month after production.

Characterization

Molecular Weight. PLA or PLA-*g*-MA resins (20 ± 5 mg) were dissolved in 10 mL high-pressure liquid chromatography (HPLC) grade tetrahydrofuran (THF) (Pharmco-Aaper, Shelbyville, KY) at ambient temperature for three days. In case of incomplete dissolution of the PLA-*g*-MA resins, the solution was heated at 40°C for several minutes, cooled, and then filtered through a 0.45 μm poly(tetrafluoroethylene) (PTFE) filter. The filtrate (100 μL) was injected into a Waters® gel permeation chromatography (GPC) equipped with a Waters® 1515 isocratic pump, a Waters® 717 autosampler, a series of Waters® Styragel columns (HR4, HR3, and HR 2), and a Waters® 2414 refractive index detector interface with Waters® Breeze software (Waters, Milford, MA.) THF was used as a mobile phase at a flow rate of 1 mL · min^{-1}.

PS standards (PS Shodex STD KIT SM 105, Showa denko, Japan) with molecular weights in the range 1.20 × 10^3 Da to 3.64 × 10^6 Da were used as external standards. The calibration curve was calculated using a third-order polynomial equation. The M_n, weight average molecular weight ($\overline{M}_w$ or M_w), polydispersity index (*PI*), and intrinsic viscosity (IV) of PLA and PLA-*g*-MA resins were determined using Waters® Breeze GPC software. *K* (0.0174 mL · g^{-1}) and *a* (0.736) values of dilute PLA solution in THF at 30°C were used to convert relative to absolute PLA M_w.[20]

Attenuated Total Reflectance-Fourier Transform Infrared (ATR-FTIR) Spectra. ATR-FTIR spectra of PLA and all blends in the form of disk specimens were acquired using an IR-Prestige 21 (Shimadzu, Columbia, MD) equipped with an Attenuated Total Reflectance (ATR) attachment (PIKE Technologies, Madison, WI). The disk specimens were stored with desiccant in a desiccator for over a week, and then the absorbance spectra were measured over the wavenumber range 4000–650 cm^{-1} at a resolution of 4 cm^{-1} with 40 consecutive scans. Three specimens were evaluated for each sample.

Thermal Degradation Temperatures. Thermogravimetric Analysis (TGA) and Derivative Thermogravimetry (DTG) thermograms were obtained using a TGA 2950 (TA Instruments, New Castle, DE). The disk specimens were cut, weighed (∼13–18 mg), and tested over the range 30–600°C at a heating rate of 10°C·min^{-1} under a N_2 atmosphere. Three replicates were tested for each sample. Thermal degradation temperatures at five percent weight loss (T_{d5}) from TGA curves and onset (T_o), maximum (T_{max}), and end decomposition (T_e) were determined from the DTG curves.

Transition Temperatures. A Differential Scanning Calorimeter (DSC) (DSC Q100, TA instruments) equipped with a refrigerated cooling system was used to determine the glass transition, cold crystallization, and melting temperatures (T_g, T_{cc}, and T_m, respectively) from the second heating scan, and crystallization temperature (T_c) from the cooling scan. Disk specimens of 8–10 mg were cut and weighed. The blend samples were heated from 25 to 175°C for the first heating scan, held at 175°C for 3 min, cooled to −50°C, and reheated to 180°C for the second heating scan, using a ramp rate of 10°C·min^{-1} under N_2 atmosphere. Three replicates were evaluated for each sample. PLA and PLA-*g*-MA were tested under the same conditions except those samples were cooled to 0°C. The degree of crystallinity (X_c) of PLA-*g*-MA or PLA in the blends was calculated according to the following equation:

$$\chi_c = \frac{\Delta H_m - \Delta H_{cc} - \Delta H_c}{\Delta H_f^* * (1-\phi)} \times 100$$

where ΔH_m, ΔH_{CC}, andΔH_C are the enthalpies of melting, cold crystallization, and crystallization, respectively, ΔH_f^* is the enthalpy of fusion of a PLA crystal of infinite size, which is 93 J·g^{-1},[21] and ϕ is the weight fraction of TPCS in the blends and/or weight fraction of MA in PLA-*g*-MA.

Dynamic Mechanical Analysis (DMA). The measurement of the storage or elastic modulus (E') and loss or viscous modulus

Table III. Extrusion and Injection Molding Conditions of Reactive Ternary Blends

PLA/PLA-*g*-MA/TPCS by weight	Extrusion condition: temperature profile (°C), screw speed (rpm), and residence time (min)	Injection molding condition: temperatures of transfer tube/mold (°C), mold residence time (s), injection pressure (psi)
63/7/30	172/172/172, 100, 5	172/38, 10, 145
56/14/30	172/172/172, 100, 5	172/38, 10, 130
35/35/30	168/168/168, 100, 5	169/38, 10, 110
14/56/30	162/162/162, 100, 5	162/38, 10, 95

Table IV. Properties of PLA-*g*-MA for Reactive Binary Blends, PLA was Used for Comparison

	PLA	PLA-*g*-MA A	PLA-*g*-MA B	PLA-*g*-MA C	PLA-*g*-MA D
M_n (kDa)	81.0 ± 8.8^{a}	70.1 ± 1.2^{a}	51.1 ± 2.9^{b}	51.4 ± 3.3^{b}	31.9 ± 2.0^{c}
M_w (kDa)	121.5 ± 2.6^{a}	110.5 ± 1.4^{b}	87.7 ± 4.3^{c}	90.7 ± 1.4^{c}	61.6 ± 0.6^{d}
PI	1.51 ± 0.14^{a}	1.58 ± 0.01^{ab}	1.71 ± 0.02^{abc}	1.77 ± 0.09^{bc}	1.94 ± 0.10^{c}
IV	0.94 ± 0.02^{a}	0.87 ± 0.01^{b}	0.73 ± 0.03^{c}	0.74 ± 0.01^{c}	0.55 ± 0.00^{d}
Grafting (%)	0^{a}	0.05 ± 0.01^{b}	0.26 ± 0.02^{c}	0.40 ± 0.00^{d}	0.47 ± 0.02^{e}
T_g (°C)	62.3 ± 0.3^{a}	62.5 ± 0.7^{a}	62.1 ± 0.5^{a}	61.5 ± 0.3^{ab}	60.9 ± 0.3^{b}
T_{cc} (°C)	118.7 ± 0.6^{a}	127.2 ± 1.0^{b}	130.5 ± 0.4^{c}	134.6 ± 1.1^{d}	133.6 ± 1.2^{d}
T_m (°C)	152.7 ± 0.8^{a}	154.5 ± 1.1^{ab}	154.6 ± 0.8^{ab}	155.2 ± 0.1^{b}	154.1 ± 0.4^{ab}
Crystallinity (%)	2.0 ± 0.9^{ab}	3.0 ± 0.6^{a}	0.5 ± 0.2^{b}	0.7 ± 0.1^{b}	1.3 ± 0.5^{b}
T_{d5} (°C)	364.6 ± 0.7^{a}	365.0 ± 2.6^{a}	364.7 ± 1.5^{a}	356.6 ± 4.5^{b}	355.9 ± 0.3^{b}
T_o (°C)	363.9 ± 1.5^{a}	365.2 ± 4.4^{a}	365.4 ± 3.1^{a}	362.6 ± 4.4^{a}	361.2 ± 3.4^{a}
T_{max} (°C)	407.4 ± 3.0^{a}	408.9 ± 2.1^{a}	410.2 ± 1.4^{a}	409.8 ± 3.4^{a}	409.3 ± 1.5^{a}
T_e (°C)	417.3 ± 3.4^{a}	420.9 ± 3.8^{a}	421.5 ± 2.1^{a}	419.0 ± 4.2^{a}	421.6 ± 2.7^{a}

Note: Numbers followed by the same letter within a row are not statistically significantly different at $P = 0.05$.

(E'') and tan delta (tan δ) as a function of time was conducted in the single cantilever mode using a DMA Q800 (TA Instruments, New Castle, DE). Bar specimens with dimensions of about 30 mm × 12.7 mm × 3 mm were conditioned at 23±2°C and 50±5% RH for not less than 60 h. Specimens were cooled from room temperature to −100°C at a ramp rate of 10°C·min^{-1}, held for 2 min, and heated to 120°C at the rate of 3°C·min^{-1}. The frequency and oscillation amplitude were 1 Hz and 30 μm, respectively. Three specimens were evaluated for each sample.

Electron Microscopy. A variable pressure scanning electron microscope (VP-SEM) EVO® LS25 (Carl Zeiss NTS, LLC, Peabody, MA) was used to evaluate fracture surfaces of the blend specimens. The bar specimens were immersed in liquid nitrogen, fractured, and mounted on aluminum stubs using adhesive tape. The micrographs were imaged under extended pressure at various magnifications.

SEM was also used to investigate the morphology of etched samples, which were prepared as follows. The bar specimens were notched using a notching cutter (Testing Machines, Islandia, NY) and impact fractured with a 2.268 kg pendulum at ambient temperature. The impact fractured samples were etched using hydrochloric acid (HCl, 6N) for 3 h to remove the TPCS phase, generating surface contrast.[22] The etched samples were air-dried in a hood, stored with desiccant for at least one day, mounted on aluminum stubs with carbon adhesive tape, and then gold-coated using an Emscope SC500 sputter coater (Emscope Laboratories, Ashford, UK). SEM images were obtained with a SEM JSM 6400 (JOEL, Tokyo, Japan) at magnifications ×3000 and accelerating voltage of 10 kV.

Tensile Properties. Tensile properties of dumbbell specimens with gage dimensions of 30 mm × 12.7 mm × 3 mm and initial grip distance of 25.4 mm were evaluated using a Universal Testing Machine (United Calibration Corp. and United Testing Systems, Huntington Beach, CA). Specimens were conditioned at 23 ± 2°C and 50 ± 10% RH for not less than 48 h. The measurement was carried out with a load cell of 4.45 kN, a crosshead speed of 2.54 mm · min^{-1}, and five specimens were evaluated for each sample.

Statistical Analysis

ANOVA and statistical mean comparisons using Tukey's HSD (Honestly Significant Difference) were analyzed using JMP® 10 software program from SAS Institute (SAS Institute, Raleigh, NC).

RESULTS AND DISCUSSION

Properties of PLA-g-MA Used in the Binary Blends

PLA-*g*-MAs with different M_n (i.e., about 70, 50, and 30 kDa) were used to blend with TPCS at a ratio of 70/30 (w/w). The M_n, grafted MA (%), and thermal properties of the PLA-*g*-MAs are listed in Table IV. PLA-*g*-MA C, with M_n similar to PLA-*g*-MA B (about 50 kDa), was specially used to investigate the effects of MA content (functionality level) on the properties of the reactive binary blends (i.e., PLA-*g*-MA and TPCS) at a particular M_n (∼ 51 kDa). Since the dominant side reaction during melt phase free radical grafting is degradation of the polymer backbone or chain scission,[23] PLA-*g*-MA with a higher degree of actual grafting had lower molecular weight and higher PI value (Table IV). Some protection from chain degradation may be obtained by using catalysts to lower the activation energy of the grafting reaction, protecting the polymer chains. The IV values of PLA-*g*-MAs are better correlated to the M_w than to the M_n and PI values; the higher M_w raised the IV. A detailed discussion of the effects of MA, L101, and screw speed (residence time) on the molecular weight properties and stability of the functionalized PLA including the optimum processing variables for producing maleated PLA can be found elsewhere.[19]

PLA and PLA-*g*-MAs did not show crystallization peaks during cooling at 10°C·min^{-1}, indicating a slow crystallization rate of both samples. The T_{cc} values of PLA-*g*-MAs significantly

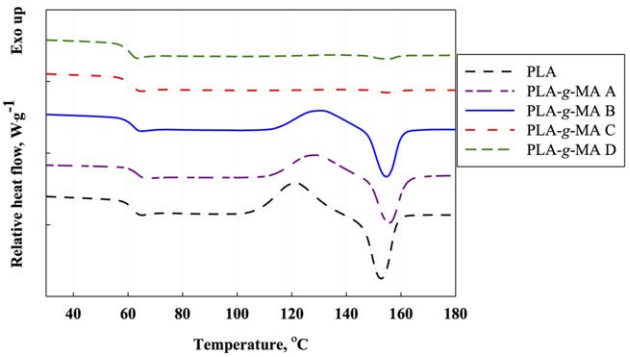

Figure 1. DSC thermogram of PLA and PLA-*g*-Mas. [Color figure can be viewed in the online issue, which is available at wileyonlinelibrary.com.]

increased with an increase of grafted MA and then gradually leveled off (Table IV). The T_g values of PLA-*g*-MAs slightly decreased from 62.5 to 60.9°C with increase of MA content. PLA and PLA-*g*-MAs for all practical purposes were amorphous (Figure 1). Changes in the transition temperatures and enthalpy of fusion are influenced by competing factors. Decreasing molecular weight of the polymer backbone improves its segmental mobility resulting in a reduction of T_g but also increasing the degree of order, which may facilitate crystallization.[24] Decrease of M_n and increase of MA was accompanied by a reduction of T_g. A slight crystallization decrease was observed with a higher degree of M_n reduction. Addition of the bulky MA group into the polymer backbone retards the chain folding, resulting in an increase of T_{cc} values.[25] Similar results (i.e., dramatic increase of T_{cc} and slight raise of T_m) were observed from MA-grafted PBAT (MA-*g*-PBAT) made by reactive extrusion.[26]

The TGA curves of PLA and PLA-*g*-MAs exhibited a single-stage decomposition reaction as later shown in Figure 3. There were no significant differences between T_o, T_{max}, and T_e values of PLA and PLA-*g*-MAs (Table IV). PLA-*g*-MAs having $\geq$ 0.4 wt % grafted MA had T_{d5} values considerably lower than the other samples ($\sim$ 8°C). The significant difference of T_{d5} values between PLA-*g*-MA B and C implies that highly grafted MA had an adverse impact on thermal stability.[27]

It is noteworthy that the thermal stability of polymer-*g*-MAs diverges, depending on grafting methods, conditions, and formulations. For example, a significant improvement of T_o for PLA-*g*-MA by about 94°C was reported when PLA/MA/benzoyl peroxide (25/15/1 by weight) were solution grafted for 4 h without noticeable differences between molecular weights of the PLA (M_n = 23.2 kDa, M_w = 28 kDa) and PLA-*g*-MA (M_n = 23.3 kDa, M_w = 28.6 kDa).[28] Chiang and Ku[29] reported that a longer solution grafting reaction ($\geq$ 60 min) increased the initial decomposition temperature of MA-grafted plasma-treated low-density PE (LDPE). Carlson *et al.*[30] found lower thermal stabilities of PLA-*g*-MAs than of PLA by 2 to 7°C when working with PLA-*g*-MAs having M_n of 83.2 to 101 kDa prepared by reactive extrusion grafting using 2 wt % MA and 0.1–0.5 wt % L101 @ 180 or 200°C.

Infrared (IR) Spectra of Reactive Binary Blends

The infrared (IR) spectrum of the physical PLA/TPCS blend (7PT) at a ratio of 70/30 by weight [Figure 2(a,b)] shows broad

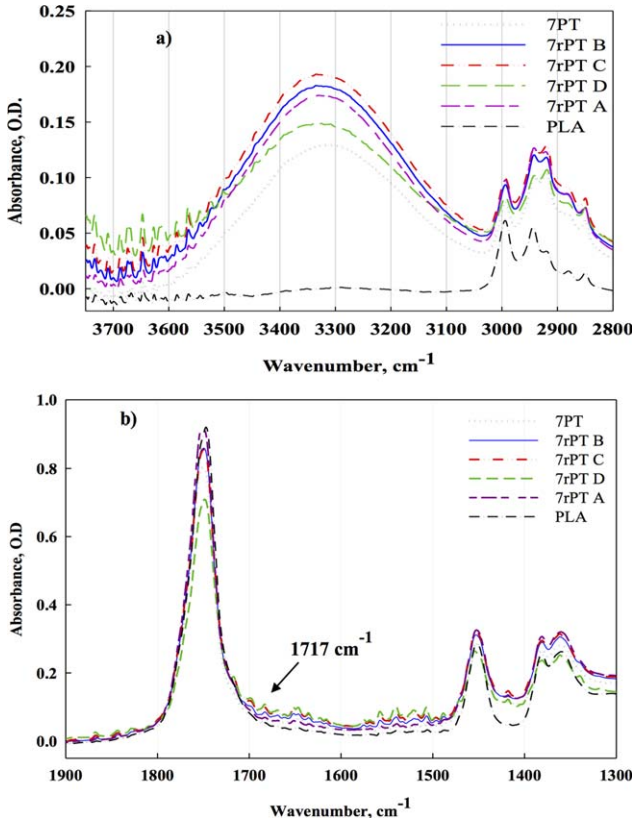

Figure 2. IR spectra of PLA, physical (7PT) and reactive blends (7rPT A, B, C, and D); (a) between 3750 and 2800 cm^{-1} and (b) between 1900 and 1300 cm^{-1}. [Color figure can be viewed in the online issue, which is available at wileyonlinelibrary.com.]

TPCS peaks at above 3000 cm^{-1} which were ascribed to the O—H stretching of inter- and intra-molecular bonding of the hydroxyl groups of the starch, and the combination of PLA peaks below 2000 cm^{-1}. The peak at 2920 cm^{-1} was attributed to the C—H stretching of CH_2 of starch.[31,32] Some PLA peaks in 7PT slightly shifted to a lower wavenumber, a red shifting, attributed to the amorphous phase of PLA (shifted from 868 to 864 cm^{-1}), and C—H stretching of $CH_{3(sym)}$ (shifted from 2943 to 2941 cm^{-1}).[33] Blue shifting, a shift to higher wavenumber due to decreased intermolecular interaction between polymer pairs, was observed from the peaks that contributed to the helical backbone vibrations with CH_3 rocking (shifted from 955 to 957 cm^{-1}), C—O in —CH—O stretching (shifted from 1180 to 1182 cm^{-1}), and C=O stretching (shifted from 1748 to 1751 cm^{-1}).[33]

The IR spectrum of 7rPT A was similar to the blend without reactive compatibilizer (7PT) except some new peak signals appeared at above 3500 cm^{-1} [Figure 2(a)]. Furthermore, the number of new peaks emerging above 3500 cm^{-1} increased with increasing grafted MA. The blue shifting of some peaks was observed in the reactive blends having $\geq$ 0.26 wt % grafted MA i.e. —CH— deformation bending (shifted from 1360 to 1362 cm^{-1}), and with the reactive blends having $\geq$ 0.4 wt % MA, i.e. —CH_3 bending (shifted from 1452 to 1454 cm^{-1}) [Figure 2(b)].[34]

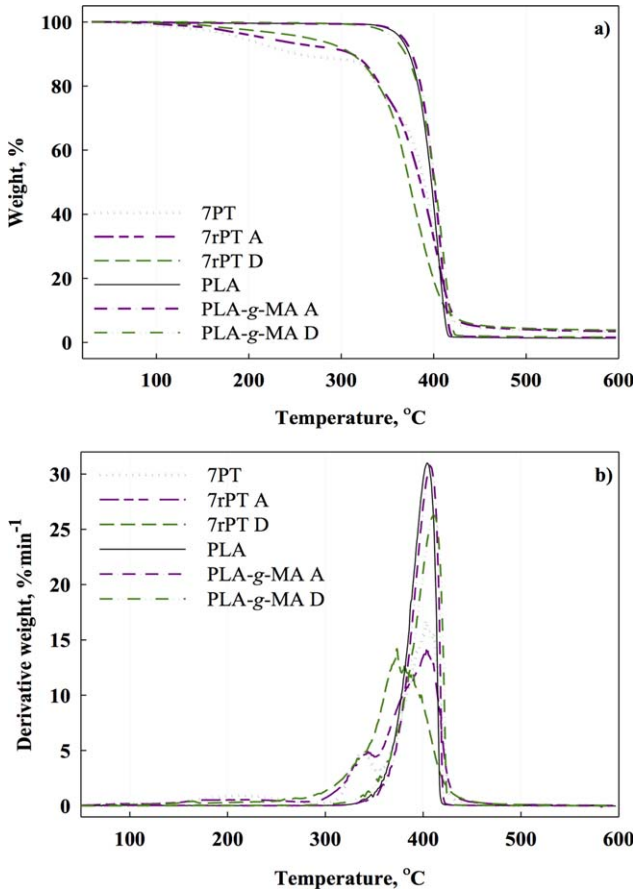

Figure 3. Thermal stabilities of physical blend, reactive blends, and PLA; (a) TGA thermogram and (b) DTG thermogram. [Color figure can be viewed in the online issue, which is available at wileyonlinelibrary.com.]

A similar trend was also observed when the reactive blends had ≥ 0.4 wt % grafted MA, the amorphous peak emerged at 866 cm^{-1} whereas the amorphous peak of PLA is located at 868 cm^{-1} (figure not shown). Several small intensity peaks appeared around 1300 to 1717 cm^{-1} in the reactive blends having ≥ 0.4 wt % grafted MA [Figure 2(b)]. Among these peaks, the one at 1717 cm^{-1} could be attributed to the carboxyl groups of hydrolyzed anhydride on PLA-*g*-MAs, which occurred when the anhydride groups of PLA-*g*-MAs interacted with the hydroxyl groups of starch (and/or glycerol) from TPCS polymer to form ester linkages as shown in Scheme 1.[9] These carboxyl groups of the hydrolyzed anhydrides could also form hydrogen bonds with the hydroxyl groups of the starch and/or glycerol.

Interactions between hydroxyl groups and anhydride groups in the other reactive blends were readily observed with FTIR technique. For example, new absorption peaks due to ester carbonyl stretching from ester linkages were investigated at 1728, 1739, and 1752 cm^{-1} in the reactive blends of LDPE/starch/PE-grafted MA (PE-*g*-MA), PCL-grafted MA/starch, and polyethylene-octene elastomer (POE)/POE-MA/starch, respectively.[35–37] The small peak observed at 1709 cm^{-1} in the LDPE/starch/PE-*g*-MA blends was due to carboxyl groups of hydrolyzed anhydrides obtained from esterification.[35]

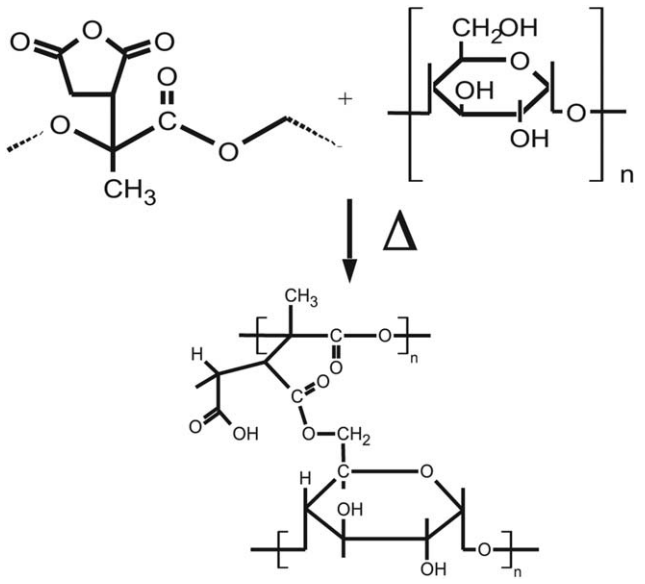

Scheme 1. Esterification of anhydride group from PLA-*g*-MA and hydroxyl group from starch.[9]

Thermal and Dynamic Mechanical Properties of Reactive Binary Blends

7PT showed multi-stage decomposition [Figure 3(a,b)], degradation around 100°C, a broad peak around 150 to 260°C, and peaks at 338 and 403°C, which were related to water evaporation, volatilization of free and bound glycerol, and decomposition of starch and PLA, respectively. Reactive blending of TPCS with PLA-*g*-MAs resulted in increased thermal stability at about 100 to 320°C, and thermal degradation at around 350 to 410°C, compared to 7PT [Figure 3(a)]. Significant differences in thermal stability properties between PLA and PLA-*g*-MAs were observed with an increase of grafted content (Table V).

Overall, the narrowing of glycerol peaks with the shift to lower temperatures, the broadening of starch peaks to 250–300°C, the overlap of starch and PLA peaks, and the shift of PLA peaks to lower temperatures were enhanced with an increase of grafted MA and a lower molecular weight of PLA-*g*-MAs [Figure 3(b)]. Complete overlapping between starch and PLA peaks was observed with PLA-*g*-MAs having high grafted MA (≥ 0.4 wt %) ([Figure 3(b)] and Table V). Interestingly, the considerable changes in T_{max} values of the starch and PLA peaks between PLA-*g*-MA B and MA C, which had the same M_n, may indicate that the increase in grafted MA is the major cause of the degradation of PLA and an overlap of PLA and starch peaks.

The improvement of thermal stability of about 100 to 320°C and the increase in degradation temperature from about 350 to 410°C found in the binary reactive blends increased with an increase of grafted MA. The higher grafted MA could enhance the interfacial adhesion between the polymer pairs resulting in better thermal stability; meanwhile, the higher grafted MA could increase the thermal degradation of PLA-*g*-MA under high temperature/pressure/shear during reactive extrusion. Similar results (i.e., improvement of T_{d5} and the shifting of the TPS peak to higher temperature and the reduction of the PLA peak to lower

Table V. T_{max} of the Physical and Reactive Blends

	T_{max} (°C)			
	Water peak	Glycerol peak	Starch peak	PLA peak
7PT	103.0 ± 3.0^{a}	213.3 ± 3.3^{a}	338.2 ± 3.1^{a}	402.9 ± 1.7^{a}
7rPT A	101.7 ± 1.9^{a}	197.0 ± 24.4^{ab}	341.5 ± 2.1^{a}	400.2 ± 3.4^{a}
7rPT B	102.9 ± 2.5^{a}	171.5 ± 3.8^{bc}	343.6 ± 4.6^{a}	400.1 ± 2.1^{a}
7rPT C	105.0 ± 2.9^{a}	166.1 ± 1.2^{c}	-	392.7 ± 2.5^{b}
7rPT D	105.3 ± 3.7^{a}	164.2 ± 1.5^{c}	-	373.8 ± 0.7^{c}

Note: Numbers followed by the same letter within a column are not statistical significant different at $P \leq 0.05$.

temperature after reactive blending) were observed from a one-step reactive extrusion blend of TPS/PLA/MA/DCP (dicumyl peroxide) at a ratio of 50/50/0.5/0.05 by weight.[5]

The enhanced partial miscibility of the polymer blends is readily indicated by the reduction of the polymer pair's T_gs.[8] Unfortunately, the low content of TPCS (30 wt %) resulted in a very low change in heat capacity (ΔC_p), so the T_gs of glycerol and starch in the blends could not be detected by DSC. Previous work by the authors showed that TPCS polymer containing 30 wt % of glycerol content had T_gs of glycerol and starch of around −47 and 60°C, respectively as determined by DSC.[6] The reduction of PLA's T_g in the physical blend (7PT) by about 2°C (Table VI) may be due to some degree of miscibility or the plasticization effect of glycerol.[38] All the reactive blends had PLA T_g values significantly lower than PLA and 7PT, especially 7rPT D having the highest grafted MA content and the lowest M_n. Lower molecular weight chains could improve the segmental mobility of PLA, and MA also acted as a plasticizer, reducing the T_g of PLA in the reactive blends as previously demonstrated.[13]

Either physical or reactive blending of PLA with TPCS resulted in no crystallization peak for PLA during cooling at 10°C·min^{-1}. A dramatic increase of PLA's T_{cc} and decrease of PLA's ΔH_{cc} was observed in the physical blend (7PT), whereas the T_{cc} values of the reactive blends decreased with an increase of grafted MA and then leveled off (Table VI). However, the ΔH_{cc} values of the reactive blends were not affected by grafting of MA and low M_n. The presence of low molecular weight agents such as plasticizers, coupling agents, and low molecular weight polymers facilitates segmental movement of high molecular weight chains, resulting in a decrease of transition temperatures, whereas chemical interactions with grafted MA reduce the segmental mobility of the polymer.[13,39,40] This could explain why an improvement of segmental mobility resulted in a decrease of T_{cc} values, which were very strongly affected by an increase of grafted MA and lower M_n. At the highest grafted MA (~0.5 wt %) the chemical interactions of grafted MA with starch and/or glycerol were dominant and counteracted the segmental mobility, resulting in a leveled-off T_{cc} value.

All the reactive blends, even the reactive blends having low grafted MA (0.05 wt %), exhibited double melting peaks, whereas the physical blend and PLA had a single melting peak (Figure 4). The second T_m value of PLA in the 7PT sample was lower than that of PLA ($P \leq 0.05$), implying that the crystalline structure of PLA had some defects.[40] Only 7rPT A had a second T_m value slightly higher than PLA, indicating high-regularity crystals. The T_m values decreased around 0.8 to 2.1°C with a reduction of PLA-*g*-MAs' M_n, whereas the first T_m values of PLA in the reactive blends significantly decreased with an increase of grafted MA, indicating that grafted MA and their M_n could be responsible for the lower temperature crystal formation (Table VI). The double melting peak behavior was also observed in additive-free poly(L-lactide) (PLLA) resin, PLA/thermoplastic acetylated starch blends, compatibilized blends of PLA/starch, PLA composites, and other structures.[13,41–44] According to Radjabian *et al.*,[45] there are three main mechanisms that can be responsible for the double-melting behavior of PLLA: melt-recrystallization, dual (or multiple) lamellae populations, and dual (or multiple) crystal structures.

Table VI. Transition Properties of Physical and Reactive Blends

				T_m, °C			
	T_g (°C)	T_{cc} (°C)	ΔH_{cc} (J·g^{-1})	First	second	ΔH_m (J·g^{-1})	X_c, %
PLA	62.3 ± 0.3^{a}	118.7 ± 0.6^{a}	23.2 ± 0.5^{a}	-	152.7 ± 0.8^{bc}	25.0 ± 0.3^{abc}	2.0 ± 0.9^{ab}
7PT	60.1 ± 0.2^{b}	123.1 ± 0.8^{b}	15.6 ± 0.3^{b}	-	151.0 ± 0.1^{d}	18.4 ± 1.2^{d}	4.2 ± 1.3^{bc}
7rPT A	59.4 ± 0.3^{c}	117.3 ± 0.4^{a}	23.4 ± 0.4^{a}	147.5 ± 0.3^{a}	154.4 ± 0.3^{a}	23.6 ± 0.6^{c}	0.3 ± 0.3^{a}
7rPT B	58.9 ± 0.1^{c}	114.4 ± 0.5^{c}	22.4 ± 0.5^{a}	146.2 ± 0.4^{b}	153.8 ± 0.2^{ab}	24.4 ± 0.5^{bc}	3.0 ± 1.4^{b}
7rPT C	59.0 ± 0.1^{c}	111.3 ± 0.3^{d}	21.9 ± 0.4^{a}	145.0 ± 0.4^{c}	153.5 ± 0.3^{ab}	25.8 ± 0.1^{ab}	6.0 ± 0.5^{c}
7rPT D	57.9 ± 0.2^{d}	111.2 ± 0.6^{d}	22.9 ± 0.8^{a}	143.5 ± 0.0^{d}	152.3 ± 0.2^{cd}	26.7 ± 0.8^{a}	5.8 ± 0.3^{c}

Note: Numbers followed by the same letter within a column are not statistically significantly different at $P \leq 0.05$.

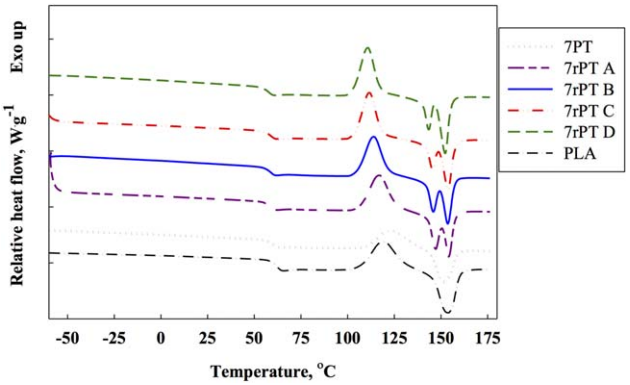

Figure 4. Crystallization and melting peaks of physical and reactive blends. [Color figure can be viewed in the online issue, which is available at wileyonlinelibrary.com.]

Among those mechanisms, melt-recrystallization (the original crystals melt during the first heating scan, and then recrystallize. The small and imperfect crystals melt at a lower melting temperature and reorganize to stable/highly regular crystals at a few degree above, and finally re-melt at the higher melting temperature) is mostly accepted as explaining the double-melting behavior of compatibilized PLA/starch blends.[13,43,44] PLLA crystallizes in three crystal forms α, β, and γ.[46] Recent studies have shown that these two melting peaks may be attributed to the crystallization of α' and α crystals formed at crystallization temperatures between 100 and 120°C.[47]

The 7PT sample also showed the lowest ΔH_m values (Table VI). The reactive blends showed ΔH_m values close to PLA which had a tendency to increase with an increase of grafted MA indicating a slight increase in crystallinity that stabilized with highly grafted MA ($\geq$ 0.4 wt %). The slight increase in crystallinity with 7rPT C, 7rPT D > 7PT > PLA could imply that TPCS acts as a nucleating agent to improve the crystallinity of PLA, and this effect is enhanced when the blends were compatibilized with highly grafted MA. This may be because the crystallization rate of PLA was increased by the addition of the TPS phase and enhanced when the blend was compatibilized with PLA-*g*-MA as previously described.[39] The effect of grafted MA on the transition temperature properties of the reactive blends is clearly seen with a comparison between 7rPT B and 7rPT C having the same M_n (Table VI). The higher grafted MA significantly decreased T_{cc} and the first T_m values, and enhanced the X_c value, indicating that compatibilization with grafted MA at up to levels of 0.4 wt % facilitated the crystallization of PLA.

Mechanical Properties and Morphology of the Reactive Binary Blends

The physical and reactive blends exhibited higher stiffness (i.e., higher E') than PLA at below −10°C, but addition of TPCS improved the flexibility of the blends at −10 to 55°C. The storage modulus of the blend decreased abruptly at about 55°C [Figure 5(a)]. The effect of functionalized PLA was clearly seen in the rubbery region of the blends (i.e., above 60°C). At above 70°C, the reactive blends, especially the 7rPT D (the reactive blend with highest grafted MA and lowest M_n), had lower stiffness compared to the physical blend (7PT), indicating that the chain mobility was increased, which could be attributed to the lower M_n of PLA-*g*-MA compared to that of PLA. The abrupt increase of E' due to the crystallization of PLA can be seen at around 84°C. The crystallization peaks of the reactive blends occurred at lower temperatures than those of PLA and 7PT, indicating that PLA crystallization was facilitated after functionalization and blending with TPCS.

The loss modulus of the physical blend (7PT), measured over the temperature range of −100 to 80°C, exhibited three transitions. The peak at about −52°C represented the T_β of the glycerol-rich domain (β relaxation), and the peak at around 4°C represented the T_α of the starch-rich domain (α relaxation), indicating the phase separation of TPCS which is normally found in typical TPS.[5] The peak at about 61°C is ascribed to the T_g of PLA. The reactive blends also exhibited the three transitions, but with the glycerol peaks shifted to a higher temperature. The peaks of the starch-rich domain of the reactive blends were broadened and overlapped more with the peaks of the glycerol-rich domain [Figure 5(b)]. The change in peak intensity was pronounced with the glycerol-rich domain, in which the peak modulus decreased with high grafted MA ($\geq$ 0.4 wt %) (Table VII), but the effects of M_n and functionality of PLA-*g*-MA on the modulus of the starch-rich domain were unclear due to the overlapping of the starch-rich domain.

While there was no significant change in PLA-*g*-MA loss modulus (Table VII), it should be noted that only the reactive blend

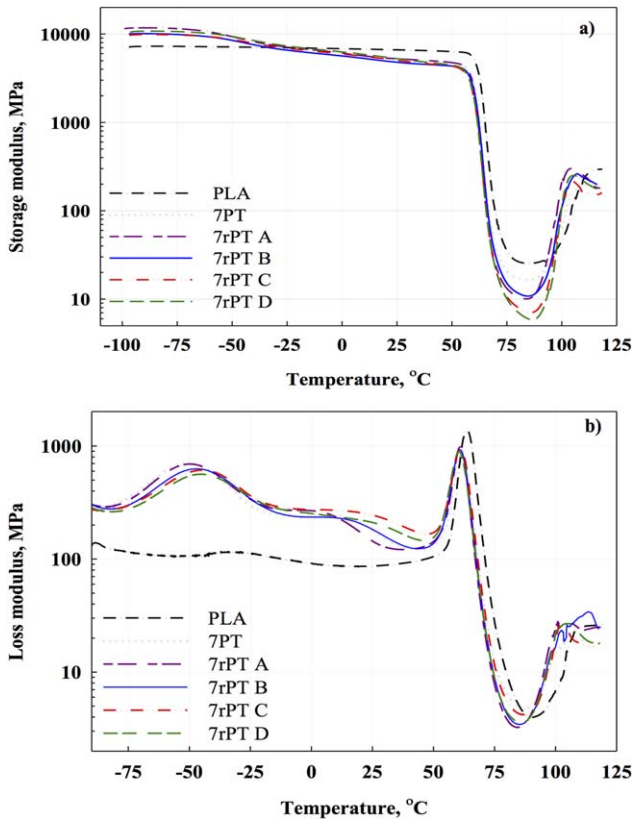

Figure 5. Storage and loss Moduli of the physical and reactive blends, (a) storage modulus and (b) loss modulus. [Color figure can be viewed in the online issue, which is available at wileyonlinelibrary.com.]

Table VII. Loss Modulus and *tan δ* Values of PLA, Physical, and Reactive Blends

	Loss Modulus (MPa)		T_gs from *Tan δ* (°C)		
	Glycerol-rich domain	PLA	Glycerol-rich domain	Starch-rich domain	PLA
PLA			-	-	68.2 ± 0.5^{a}
7PT	709.4 ± 6.1^{a}	897.9 ± 54.6^{a}	-47.2 ± 0.8^{a}	11.7 ± 1.4^{a}	66.4 ± 0.4^{b}
7rPT A	703.6 ± 28.3^{a}	945.7 ± 49.1^{a}	-46.3 ± 0.3^{a}	1.8 ± 2.2^{b}	66.3 ± 0.1^{b}
7rPT B	615.2 ± 19.7^{ab}	908.7 ± 35.3^{a}	-43.1 ± 0.5^{b}	12.8 ± 0.6^{a}	66.8 ± 0.3^{b}
7rPT C	595.2 ± 81.0^{b}	918.5 ± 58.0^{a}	-41.7 ± 0.6^{bc}	16.6 ± 6.8^{a}	66.5 ± 0.1^{b}
7rPT D	559.0 ± 17.6^{b}	876.6 ± 36.3^{a}	-41.2 ± 0.4^{c}	17.7 ± 1.6^{a}	66.4 ± 0.2^{b}

Note: Numbers followed by the same letter within a column are not statistically significantly different at $P \leq 0.05$.

having the highest grafted MA or lowest M_n (7rPT D) had a loss modulus (E'') value lower than the physical blend. A similar result was observed with PE/TPS blends compatibilized with PE-*g*-MA.[48] The addition of PE-*g*-MA, having a M_n of about 31 kDa and MA concentration of 3.9%, decreased the amplitude of T_β peaks, but the amplitude of the T_α peaks did not vary significantly with increasing of PE-*g*-MA content.

The effects of PLA-*g*-MA on shifting of T_gs were more clearly identified from the tan δ determinations than by the loss modulus due to less overlapping of the starch-rich domain with the glycerol-rich domain (data not shown). Addition of 30 wt % TPCS in PLA resulted in a decrease of PLA's T_g value by about 2°C ($P \leq 0.05$), whereas the T_gs of the glycerol-rich and starch-rich domains appeared at around −47 and 12°C, respectively (Table VII). Although there was no difference between the T_g values of PLA observed from the physical and reactive blends, there was a trend that the T_g shifts of the glycerol-rich and starch-rich domains increased with an increase of grafted MA and then leveled off at ≥ 0.4 wt % grafted MA [Figure 5(b)].

Comparing the reactive blends having different M_n and grafted MA values (7rPT A, B, and D), the increase of the T_g values of TPCS enhanced with an increase of grafted MA and a decrease of M_n of PLA-*g*-MA. Furthermore, comparison between the reactive blends having similar M_n values (7rPT C and D) showed that an increase of grafted MA increased the starch-rich domain's T_g value by about 4°C. This could be attributed to an increase in ester formation between the anhydride groups of PLA-*g*-MA and the hydroxyl groups of glycerol and starch. Therefore, the increase of TPCS' T_g values could also serve as evidence that the reactive compatibilization of PLA and TPCS via grafted MA was established.

It should also be noted that a decrease of the glycerol-rich T_gs was observed in the reactive blends having higher grafted MA (0.26 wt % with M_n of 50 kDa), whereas a increase of the starch-rich T_gs was found in the reactive blends having ≥ 0.4 wt % grafted MA with M_n of ≤ 50 kDa. Taguet *et al.*[48] also reported that MA would first interact at the interfacial glycerol-rich layer, especially with high glycerol content. This may be because glycerol has lower viscosity than starch. Hence, 0.4 wt % grafted MA of PLA-*g*-MA having M_n of 50 kDa is effective for reactive compatibilization of PLA and TPCS at a ratio of 70/30 by weight. Further SEM and tensile measurements were carried out to investigate these results.

The VP-SEM micrograph of the fracture surface of the physical blend (7PT) showed good interfacial adhesion between the TPCS domains and the PLA continuous phase as no voids were evident between the two phases. The TPCS domains had globular and irregular shapes [Figure 6(a)]. A reduction in domain size of TPCS and increase in starch chain mobility due to the plasticization effect of glycerol facilitates hydrogen-bonding between the starch and PLA.[45] Taguet *et al.*[48] investigated the effect of glycerol content on the reduction of TPS domain size in TPS/HDPE blends and found that the glycerol threshold is close to 28 wt %. Good interfacial adhesion of the physical blend was also observed from the cryogenic fracture surface of a 40/60 polycaprolactone/TPS blend, in which the glycerol content in a starch-water-glycerol suspension was 28 wt %.[49]

Marked changes in fracture surfaces of the reactive blends compared with 7PT were observed with blends having grafted MA ≥ 0.26 wt % and $M_n \leq 50$ kDa (7rPT B, C, and D) [Figure 6(b–d)]. The fracture surfaces of those reactive blends seem to be smoother. The number of small domains of TPCS increased and better dispersion was observed with an increase of grafted MA and/or decreased M_n of PLA-*g*-MA. Comparing the reactive blends having the same M_n of PLA-*g*-MA (7rPT B and C), the reactive blend having a higher grafted MA (7rPT C) exhibited a larger amount of small TPCS domains [Figure 6(b,c)]. Additional information about the effects of grafted MA and M_n of PLA-*g*-MA on TPCS domain size, shape, and dispersion was observed by removing the TPCS phase with acid etching. The dispersion of the TPCS domains in the PLA phase in the physical blend was not uniform [(Figure 7(a)]. The TPCS domains were somewhat spherical with some domains presenting irregular shapes with a high variation of domain sizes.

Interestingly, the dispersion and uniformity of TPCS domains in the PLA-*g*-MA continuous phase of 7rPT A was dramatically improved even when PLA-*g*-MA having a small amount of grafted MA (0.05 wt %) was used [Figure 7(b)]. TPCS domains of the reactive blends were nearly spherical, and TPCS domain sizes decreased noticeably with an increase of grafted MA as also shown elsewhere.[5,10] These results emphasized that reactive compatibilization in the TPCS blends existed when the

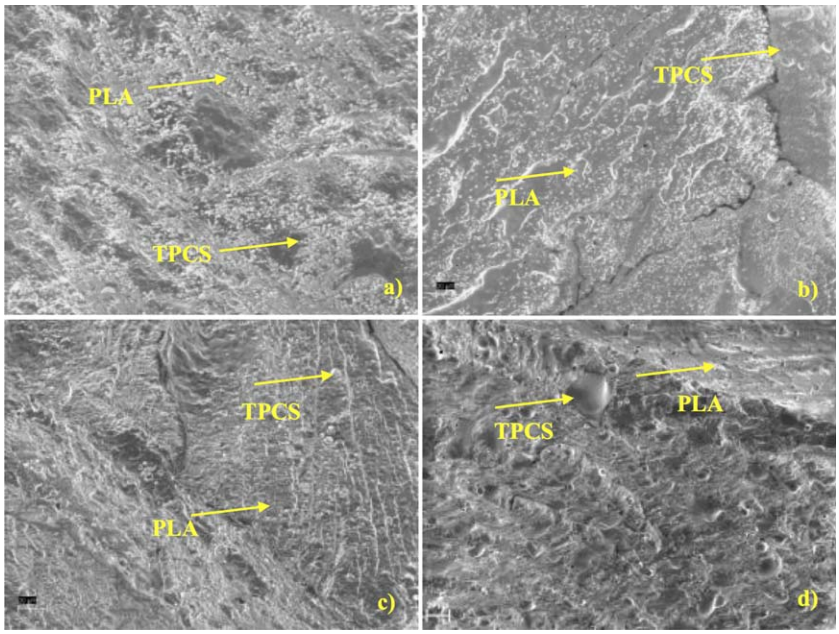

Figure 6. VP-SEM fracture surface micrographs of physical and reactive blends: (a) 7PT, (b) 7rPT B, (c) 7rPT C, and (d) 7rPT D (magnification bars are 20 μm). [Color figure can be viewed in the online issue, which is available at wileyonlinelibrary.com.]

functionalized PLA was used as a polymer pair even with a very low content of grafted MA (0.05%); hence, the mechanical properties of these reactive blends were expected to improve, as shown later on. Surprisingly, the most uniform domain size was observed with the reactive blend containing a low amount of grafted MA and a high M_n with a low PI value (7rPT A). Reactive blending of TPCS with PLA-*g*-MA containing a high amount of grafted MA content ($\geq$ 0.4 wt %) generated a large TPCS domain phase [Figure 7(d,e)]. The numbers of large TPCS domains increased with an increase of grafted MA and decreased M_n. Similar results were found in reactive two-step 27% TPS/PLA blends where 20% of the pure PLA was substituted by PLA grafted using nominal 2 wt % MA and 0.5 wt % L101.[10]

Reactive compatibilization not only lowered the interfacial tension between the two polymer phases but also suppressed the coalescence of droplets by introducing steric stabilization, resulting in a finer and more stable morphology.[50,51] However, shear- or flow-induced coalescence (dynamic coalescence) was found in compatibilized systems at sufficiently high shear rate and/or prolonged mixing due to a decrease of the polymer matrix viscosity and/ or the removal of graft copolymers from the interfaces.[52,53] The phase coalescence is enhanced with decrease in molecular weight and thus in matrix viscosity, since those factors reduced the dispersive forces at the origin of the particle break-up and the interface generation.[54] In this work, the presence of a high quantity of finer domains in the sub-micron levels with a small quantity of large domains ($\geq$ 4 μm) of TPCS in the PLA-*g*-MA matrix having high grafted MA ($\geq$ 0.4 wt %) and lower M_n ($\leq$ 50 kDa) could be related to effects of grafted MA and its M_n. An increase of grafted MA reduced the interfacial tension, resulting in finer domains, but a decrease in matrix viscosity due to the lower M_n of the PLA-*g*-MA enhanced dynamic coalescence, resulting in large domains. Furthermore, a reduction of the PLA-*g*-MA viscosities could be enhanced by an increase of chain scission produced by the high shear, high temperature, and especially high MA content during the reactive extrusion. This could be the main reason for the dynamic coalescence observed in this work, since the reactive blends (7rPT B) having similar M_n (about 50 kDa) but lower grafted MA (0.26 wt %) did not present large domains of PLA as 7rPT C did [Figure 7(c,d)]. The large domains may act as stress concentrators, which may deteriorate the sample mechanical properties. To prove this assumption, the tensile properties of 7rPT B and 7rPT C were investigated and compared to those of PLA and the physical blend. The 7rPT B and 7rPT C were selected because these two reactive blends presented noticeable inward shifts of TPCS T_gs, significant reduction of domain size, and a different presence/absence of large domains.

Ductility improvement of the physical blend (7PT) due to introduction of a ductile polymer, TPCS, into the PLA matrix was exemplified in its tensile properties. PLA, a brittle polymer, had Young's modulus, tensile strength at break, and elongation at break of 2.8 ± 0.7 GPa, 65.9 ± 1.4 MPa, and 2.8 ± 0.4%, respectively. Compared to PLA, the Young's modulus and tensile strength at break of 7PT decreased by about 43% and 28%, respectively, whereas elongation at break increased by about 1390% with an addition of 30 wt % TPCS. Blending of 30 wt % TPCS with PLA-*g*-MA having similar M_n but difference in functionality levels (grafted MA) provided reactive blends with different tensile behaviors as shown later in Figure 8. The 7rPT B blend exhibited tensile properties similar to 7PT with a slight enhancement of stiffness resulting from an improvement of interfacial chemical interactions, mainly ester linkages, between the TPCS domains and PLA-*g*-MA matrix. Compared to PLA, the tensile strength of 7rPT B decreased by about 39%, while the elongation at break increased by about 1100%.

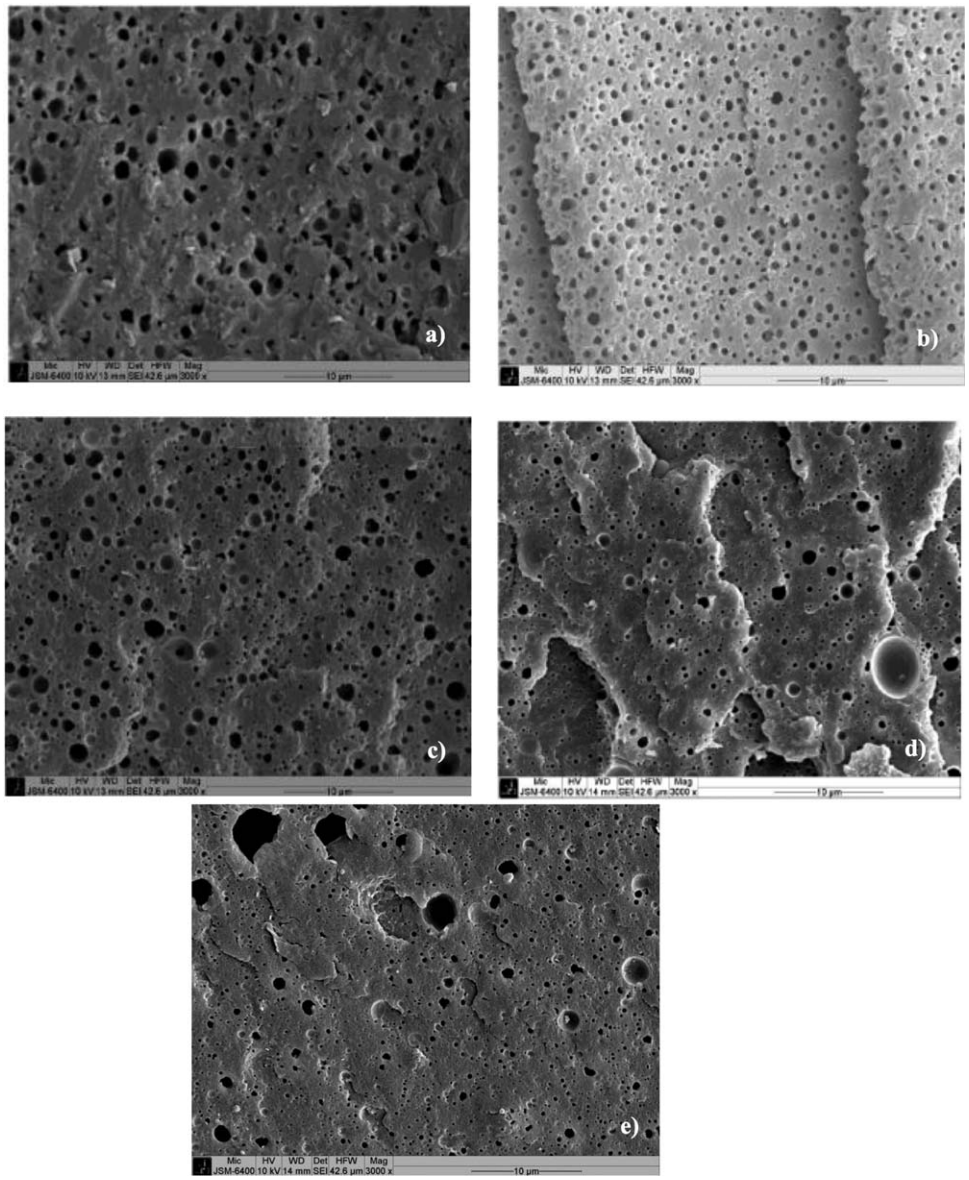

Figure 7. SEM micrographs after removing TPCS domains by acid etching of physical and reactive blends: (a) 7PT, (b) 7rPT A, (c) 7rPT B, (d) 7rPT C, and (e) 7rPT D.

As expected, an increase of grafted MA (0.4%) tremendously deteriorated the ductile properties of 7rPT C, its Young's modulus, tensile strength at break, and elongation at break compared to PLA decreased by about 14%, 53%, and 57%, respectively. Decreased tensile properties of the reactive blends due to an increase of grafted MA were also mentioned elsewhere.[9,11] In this work, the large domain size shown in Figure 7(d) may act as stress concentrators resulting in inferior tensile properties due to induced cracks and produced premature failure during the tensile testing. Further research is needed to fully explain the effect of grafted MA and M_n on the binary blend tensile properties, especially elongation at break. Better tensile properties may be achieved from the blends containing less than 0.4 wt % grafted MA. Therefore, the optimum grafted MA providing better tensile properties was further investigated by substitution of PLA content with different amounts of PLA-*g*-MA and blending with 30 wt % TPCS. The approach of creating a ternary blend was used to concentrate on the effect of grafted MA.

Tensile Properties and Morphology of Reactive Ternary Blends

For the ternary blends, a new process PLA-*g*-MA E, having grafted MA of 0.52 ± 0.02 wt % and M_n of 44.9 ± 1.0 kDa, was used as a PLA substitute since its M_n was comparable to PLA-*g*-MA B and C, but with higher grafted MA. The M_n of PLA-*g*-MA around 45–50 kDa was selected for producing the ternary blends since reactive blends produced with this amount of MA on PLA-*g*-MA showed better interfacial adhesion [Figure 7(c,d)]. Furthermore, with the higher grafted MA, the ternary reactive blends could be tailor-made to provide reactive blends having different levels of grafted MA, which would be comparable with the previous reactive binary blends. The ternary blends

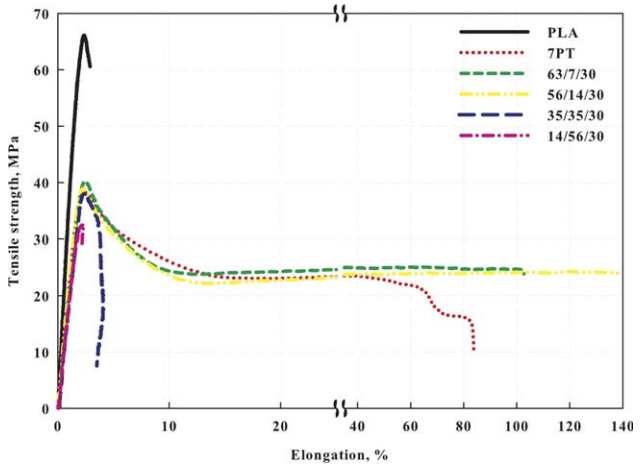

Figure 8. Tensile properties of PLA/PLA-*g*-MA E/TPCS blends, PLA, and 7PT. [Color figure can be viewed in the online issue, which is available at wileyonlinelibrary.com.]

having PLA-*g*-MA E of 7, 35, and 56 wt % had grafted MA comparable to 7rPT A, 7rPT B, and 7rPT C, respectively. Finally, the ternary blend having PLA-*g*-MA E of 14 wt % had grafted MA based on PLA-*g*-MA and PLA weights around 0.1 wt %. The tensile properties of dumbbell specimens of the reactive PLA/PLA-*g*-MA E/TPCS blends compared to PLA and 7PT are shown in Figure 8.

PLA exhibited necking without drawing. Addition of 30 wt % TPCS, a ductile component, resulted in an increase in the plastic region after the yield point with a reduction of stiffness. 7PT had tensile strength of 38.9 ± 0.4 MPa, Young's Modulus of 2.2 ± 0.2 GPa, and elongation at break of $81.2 \pm 18.2\%$. Compared to 7PT, increasing the substituted PLA-*g*-MA E content up to 35 wt % slightly improved the Young's modulus but had almost no effect on the tensile strength. However, an increase in elongation at break of the ternary blends was observed when a low amount of the PLA-*g*-MA E (up to 14 wt %) was substituted. Beyond this value the ternary blends completely lost the cold drawing characteristic (plastic region). The highest value of elongation at break, $145.1 \pm 45.6\%$, was obtained from the blends at a ratio of 56/14/30 (PLA/PLA-*g*-MA E/TPCS). This reactive ternary blend also had tensile strength of 38.9 ± 0.4 MPa and Young's modulus of 2.4 ± 0.3 GPa.

The highest amount of PLA-*g*-MA E used (56 wt %) deteriorated both strength and ductile properties of the reactive blend. This ternary reactive blend had tensile strength (32.5 ± 2.2 MPa) reduced by half compared to PLA, Young's modulus of 2.1 ± 0.2 GPa, and elongation at break $2.3 \pm 0.7\%$, less than PLA. Zhang and Sun[9] also reported that the mechanical properties of the composites were not further improved if the concentrations of grafted copolymer (compatibilizer) at the interface increased beyond a critical level. Another reason why increasing reactive compatibilizer content did not improve mechanical properties of the reactive blends could be the deterioration of intrinsic mechanical properties of PLA-*g*-MA E due to chain scission reducing its molecular weight during reactive functionalization. Similar results (i.e., blends of TPS with PLA functionalized by MA dramatically improved elongation at break but have little effect on the tensile modulus and strength) were reported by Huneault and Li.[10] In their work, the maximum increase of elongation at break of reactive TPS/PLA blends (about 205 to 185%) was obtained when PLA was completely replaced by PLA-*g*-MA made from 2 wt % MA and 0.25 wt % L101 (the grafting level was 0.8 wt %), regardless of TPS content (27, 43, and 60 wt %). However, in this work the highest elongation at break of the 70 wt % PLA and 30 wt % TPCS was observed when 20 wt % PLA was replaced by PLA-*g*-MA having 0.52 wt % grafted MA. This clearly shows the effectiveness of PLA-*g*-MA as a reactive compatibilizer for PLA and TPCS blends. Only the low grafted MA was essential and sufficient to produce a finer and more stable morphology, resulting in an improvement of tensile properties of the final ternary blends. The etched SEM micrographs of the reactive ternary blends (Figure 9) revealed that the more uniform tensile properties (56/14/30) resulted not only from the better dispersion of TPCS domains, the smaller domain sizes, and the stable morphology, but also from the narrow distribution of domain sizes [Figure 9(c)].

Furthermore, it was evident that the reactive blends having 0.4 wt % grafted MA either used in the form of a functional polymer pair (binary blend: 7rPT C) or used in the form of reactive compatibilizer (ternary blend: 14/56/30) exhibited poor tensile properties compared to PLA and the physical blend. Interestingly, the reactive blend having about 0.26 wt % grafted MA in the form of a binary blend (7rPT B) had better tensile properties, closer to those of the physical blend than the ternary blend (35/35/30), which exhibited tensile strength of 32.5 ± 2.2 MPa, Young's modulus of 2.1 ± 0.2 GPa, and elongation at break of 4.6%. This may be because the reactive binary blend [Figure 7(c)] had a narrower distribution of TPCS domain sizes than the reactive ternary blend [Figure 9(d)]. In comparing the reactive blends having 0.05 wt % MA content, the reactive binary blend, 7rPT A, showed better dispersion and a finer morphology than the reactive ternary blend, 63/7/30 [Figures 7(b), 9(b)]. It is noteworthy that functionalized PLA used in the 7rPT A blends, PLA-*g*-MA A, had higher M_n (about 70 kDa) than the one used in the 63/7/30, PLA-*g*-MA E having M_n of about 45 kDa.

The tensile properties and blend morphologies indicated that the functionality level (grafted MA level on PLA) of PLA-*g*-MA played an important role in improving the dispersion of TPCS domains, controlling TPCS particle sizes and distribution of domain sizes, and finally stabilizing the domains. As a consequence, the compatibility between the polymers in the blend, and hence the tensile properties, were improved. However, 7rPT A had a finer morphology than the 63/7/30. Those reactive blends had similar MA content but differed in M_n of PLA-*g*-MA. Therefore, the molecular weight of PLA-*g*-MA may be another parameter that has a significant effect on controlling the morphology and mechanical properties of the final reactive blends.

To prove this assumption, PLA-*g*-MA having a similar functionality level as PLA-*g*-MA E (0.52 ± 0.02 wt % grafted MA) but differing in M_n was investigated. Unfortunately, PLA-*g*-MA having 0.5 wt % grafted MA and higher M_n ($\geq$ 60 kDa) could not be produced by simple reactive functionalization of PLA/MA/

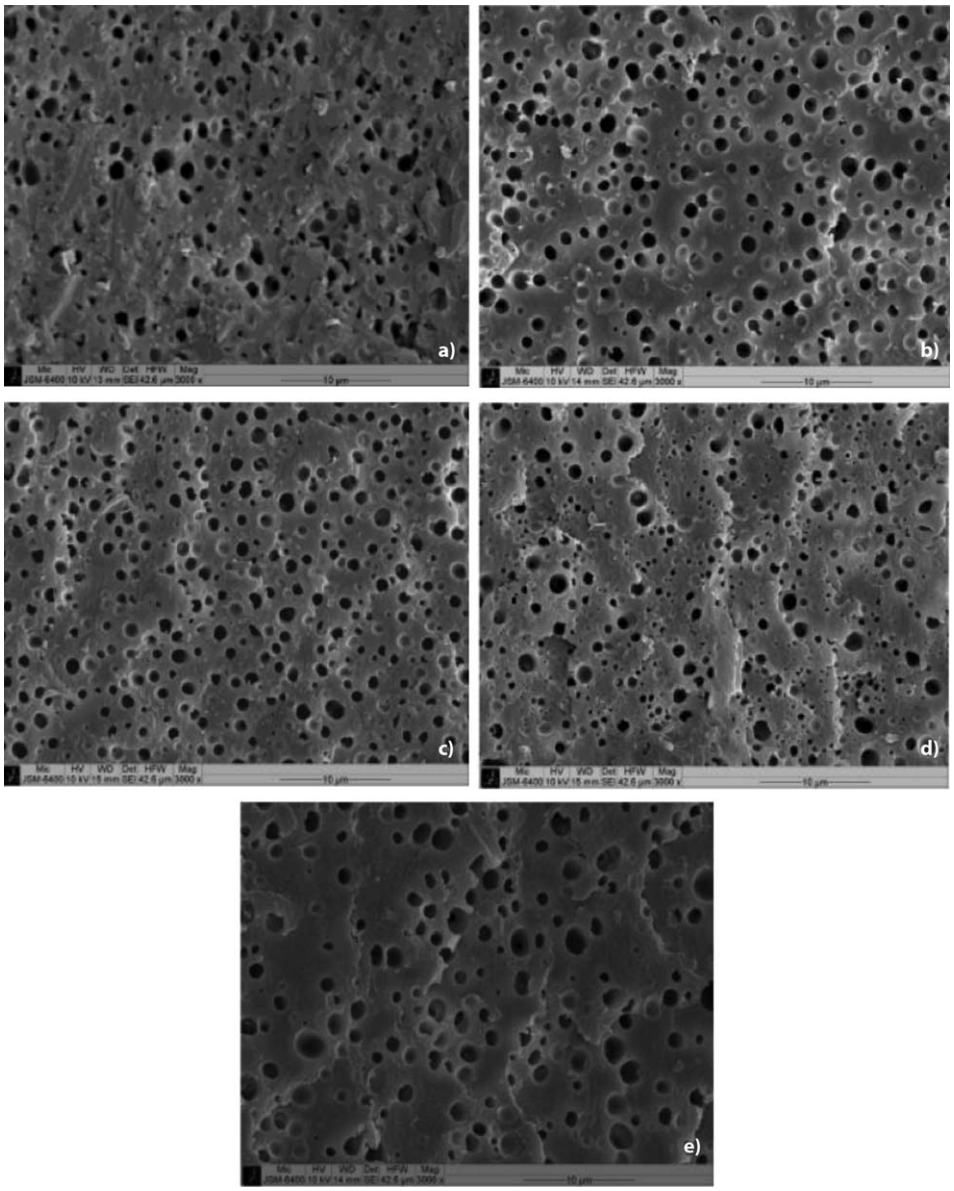

Figure 9. Etched SEM micrographs of binary and ternary blends: (a) 7PT, (b) 63/7/30 of PLA/PLA-*g*-MA E/TPCS, (c) 56/14/30 of PLA/PLA-*g*-MA E/TPCS, (d) 35/35/30 of PLA/PLA-*g*-MA E/TPCS, and (e) 56/14/30 of PLA/PLA-*g*-MA F/TPCS.

L101 since an increase of MA resulted in a higher amount of grafted MA with a reduction of grafted PLA molecular weight.[19] Hence, only PLA-*g*-MA F having grafted MA of 0.50 ± 0.02 wt % and M_n of 15.0 ± 1.9 kDa was further used to prepare the ternary blends at the ratios of 63/7/30 and 56/14/30 since these ratios provided the better tensile properties of the ternary blends compared to the physical blend. The 63/7/30 PLA/PLA-*g*-MA F/TPCS blend had a tensile strength of 40.8 ± 0.5 MPa, Young's modulus of 2.6 ± 0.4 GPa, and elongation at break of 16.2 ± 14.7%. Increasing PLA-*g*-MA F to 14 wt % tremendously diminished the ductility of the final blend. The 56/14/30 blend exhibited a tensile strength of 38.6 ± 0.7 MPa, Young's modulus of 2.2 ± 0.4 GPa, and elongation at break of 3.1 ± 0.7%. Compared with the ratio that provided the best mechanical properties (14 wt % of PLA-*g*-MA E) and the physical blend (Figures 9(c,a), respectively), the etched morphology of the reactive ternary blend containing 14 wt % PLA-*g*-MA F [Figure 9(e)] had a poorer distribution of TPCS domains with slightly bigger TPCS domain sizes than those of the reactive blend containing 14 wt % of PLA-g-MA E. Thus, it can be stated that the M_n of PLA-*g*-MA had a significant effect on controlling the morphology and tensile properties of the reactive PLA/TPCS blends. The distribution of the TPCS domains, the decrease of domain sizes, the finer morphology, and then the tensile properties were enhanced with the higher M_n of PLA-*g*-MA when the same amounts at a low concentration of PLA-*g*-MA were used. Similar results were found by Park *et al.*[55] that 5 wt % high molecular weights of functionalized PS with MA (M_n of 100 to 125 kDa) were more effective in decreasing and stabilizing the dispersed domain size of PA6 and PS blends than the low

molecular weight ones (M_n of 15 to 68 kDa). They also observed that the adhesion strength increased with the addition of high M_w functionalized PS.[55] Thus, adding PLA-*g*-MAs having grafted MA of 0.52 ± 0.02 wt % and M_n of 44.9 ± 1.0 kDa at 14 wt % was effective as a reactive compatibilizer or reactive (functionalized) polymer of biodegradable ternary blends of PLA/ TPCS.

CONCLUSIONS

PLA-*g*-MA having grafted MA of 0.05 to 0.47 wt % and M_n of about 70 to 30 kDa exhibited transition temperatures close to PLA, but the cold crystallization temperature values of PLA-*g*-MA increased with an increase of grafted MA and then leveled off. A new IR peak at 1717 cm^{-1}, reduction of PLA's T_g, and increase of T_g values of the glycerol were found especially from the reactive binary blends of 30 wt % TPCS and 70 wt % PLA-*g*-MA having high grafted MA, indicating that chemical interactions between anhydride groups of PLA-*g*-MA and hydroxyl groups of starch and glycerol were present. The formation of these ester linkages resulted in a decrease of interfacial adhesion between PLA-*g*-MA and TPCS phases, a reduction of TPCS domain sizes and an improvement of domain dispersion and uniform morphology even for blends having a low grafted MA content (0.05 wt % on PLA basis). Compared to the physical blends, the reactive binary blends showed smaller TPCS domains with an increase of grafted MA, but at MA $\geq$ 0.4 wt % a number of large TPCS domain sizes were present, deteriorating the tensile strength and elongation at break of the binary blends. The reactive ternary blends exhibited the same trend as the reactive binary blends (i.e., increasing grafted MA improved TPCS dispersion and lowered TPCS domain sizes). Broader TPCS domain size and poor tensile properties were observed in reactive blends having $\geq$ 0.26 wt % grafted MA (35/35/30 by weight of PLA/PLA-*g*-MA E/TPCS). Reactive compatibilizer had a strong impact on flexibility, but did not affect modulus and tensile strength. The highest (optimum) elongation at break was observed in the reactive blend having 0.1 wt % grafted MA (PLA basis), with the reactive compatibilizer having a M_n of 45 kDa. PLA-*g*-MA having similar grafted MA but higher M_n offered noticeably better TPCS dispersion, a finer and more uniform morphology, and also a larger elongation at break. Thus, PLA-*g*-MA is very effective as a reactive polymer pair or reactive compatibilizer with TPCS when PLA is used as a main component. The use of PLA-*g*-MA having 0.1 wt % grafted MA and M_n not less than 45 kDa as a reactive polymer can improve the morphology and mechanical properties of TPCS blends, and help to successfully develop industrially compostable blends of TPCS and PLA. The blends showed high elongation at break with minimal reduction of tensile strength, so they can be used for industrial flexible applications such as packaging and agriculture films. Further, research is needed to determine the optimal processing conditions for the blends to control the homogeneity of the grafted MA onto PLA and the side reactions occurring during extrusion and the stability of these blends during storage. Final assessment of the biodegradability of these blends should be conducted. All these data should be combined to fully evaluate the potential applications for this reactive material before full scale production.

ACKNOWLEDGMENTS

S.D. thanks the Royal Thai government, the PET Amcor fellowship, the SoP graduate fellowships for financial support. R.A. thanks the partial support of the USDA National Institute of Food and Agriculture and Michigan AgBioResearch, Hatch project R. Auras. The authors thank Erawan Marketing and Chemtura for providing the cassava starch, and L. Matuana for helping with the production of the PLA-*g*-MA.

REFERENCES

1. Auras, R.; Harte, B.; Selke, S. *Macromol. Biosci.* **2004**, *4*, 835.
2. Lim, L. T.; Auras, R.; Rubino, M. *Progr. Polym. Sci.* **2008**, *33*, 820.
3. Detyothin, S.; Kathuria, A.; Jaruwattanayon, W.; Selke, S. E. M.; Auras, R., Eds. Poly(lactic acid) Blends; Wiley: Hoboken, **2010**.
4. Yu, L.; Petinakis, E.; Dean, K.; Liu, H., Eds. Poly(lactic acid)/starch Blends; Wiley: Hoboken, **2010**.
5. Wang, N.; Yu, J. G.; Ma, X. F. *Polym. Int.* **2007**, *56*, 1440.
6. Detyothin, S. Production and Characterization of Thermoplastic Cassava Starch, Functionalized Poly(lactic acid), and Their Reactive Compatibilized Blends. Ph.D. Thesis, School of Packaging; Michigan State University: East Lansing, MI, **2012**; p 257.
7. Baker, W.; Scott, C.; Hu, G.-H., Eds. Reactive Polymer Blending; Hanser: Munich, **2001**.
8. Robeson, L. M., Ed. Polymer Blends: A Comprehensive Review; Carl Hanser Verlag: Munich, **2007**.
9. Zhang, J. F.; Sun, X. Z. *Biomacromolecules* **2004**, *5*, 1446.
10. Huneault, M. A.; Li, H. B. *Polymer* **2007**, *48*, 270.
11. Wang, S. J.; Yu, J. G.; Yu, J. L. *Polym. Degrad. Stab.* **2005**, *87*, 395.
12. Maliger, R. B.; McGlashan, S. A.; Halley, P. J.; Matthew, L. G. *Polym. Eng. Sci.* **2006**, *46*, 248.
13. Jang, W. Y.; Shin, B. Y.; Lee, T. X.; Narayan, R. *J Ind. Eng. Chem.* **2007**, *13*, 457.
14. Raquez, J. M.; Nabar, Y.; Narayan, R.; Dubois, P. *Polym. Eng. Sci.* **2008**, *48*, 1747.
15. Prachayawarakorn, J.; Sangnitidej, P.; Boonpasith, P. *Carbohydr. Polym.* **2010**, *81*, 425.
16. Jo, W. H.; Park, C. D.; Lee, M. S., *Polymer* **1996**, *37*, 1709.
17. Ozturk, C.; Kusefoglu, S. H. *J. Appl. Polym. Sci.* **2010**, *118*, 3311.
18. Clark, D. C.; Baker, W. E.; Whitney, R. A. *J. Appl. Polym. Sci.* **2001**, *79*, 96.
19. Detyothin, S.; Selke, S. E. M.; Narayan, R.; Rubino, M.; Auras, R. *Polym. Degrad. Stabil.* **2013**, *98*, 2697.
20. Dorgan, J. R.; Janzen, J.; Knauss, D. M.; Hait, S. B.; Limoges, B. R.; Hutchinson, M. H. *J. Polym. Sci. Pol. Phys.* **2005**, *43*, 3100.

21. Fischer, E. W.; Sterzel, H. J.; Wegner, G.; Kolloid-Z.u.Z, *Polymere* **1973**, *251*, 980.
22. Li, H. B.; Huneault, M. A. *J. Appl. Polym. Sci.* **2011**, *122*, 134.
23. Cha, J.; White, J. L. *Polym. Eng. Sci.* **2001**, *41*, 1227.
24. Chen, C.; Peng, S. W.; Fei, B.; Zhuang, Y. G.; Dong, L. S.; Feng, Z. L.; Chen, S.; Xia, H. M. *J. Appl. Polym. Sci.* **2003**, *88*, 659.
25. Fontana, G.; Minto, F.; Gleria, M.; Facchin, G.; Bertani, R.; Favero, G., *Eur. Polym. J.* **1996**, *32*, 1273.
26. Nabar, Y.; Raquez, J. M.; Dubois, P.; Narayan, R., *Biomacromolecules* **2005**, *6*, 807.
27. Domenichelli, I.; Coiai, S.; Cicogna, F.; Pinzino, C.; Passaglia, E. *Polym. Int.* to appear DOI 10.1002/pi.4799. http://onlinelibrary.wiley.com/doi/10.1002/pi.4799/abstract.
28. Plackett, D. *J. Polym. Env.* **2004**, *12*, 131.
29. Chiang, W. Y.; Ku, Y. A. *Polym. Degrad. Stabil.* **2002**, *76*, 281.
30. Carlson, D.; Nie, L.; Narayan, R.; Dubois, P. *J. Appl. Polym. Sci.* **1999**, *72*, 477.
31. Shi, R.; Liu, Q. Y.; Ding, T.; Han, Y. M.; Zhang, L. Q.; Chen, D. F.; Tian, W. *J. Appl. Polym. Sci.* **2007**, *103*, 574.
32. Kim, D. H.; Na, S. K.; Park, J. S. *J. Appl. Polym. Sci.* **2003**, *88*, 2108.
33. Goncalves, C. M. B.; Coutinho, J. A. P.; Marrucho, I. M., Eds. Optical Properties; Wiley: Hoboken, **2010**.
34. Guan, J.; Hanna, M. A. *Ind. Eng. Chem. Res.* **2005**, *44*, 3106.
35. Bikiaris, D.; Panayiotou, C. *J. Appl. Polym. Sci.* **1998**, *70*, 1503.
36. Wu, C. S. *Polym. Degrad. Stab.* **2003**, *80*, 127.
37. Fu, X.; Chen, X. D.; Wen, R. G.; He, X. W.; Shang, X. Y.; Liao, Z. F.; Yang, L. S. *J. Polym. Res.* **2007**, *14*, 297.
38. Park, J. W.; Im, S. S.; Kim, S. H.; Kim, Y. H. *Polym. Eng. Sci.* **2000**, *40*, 2539.
39. Li, H.; Huneault, M. A. *Int. Polym Proc.* **2008**, *23*, 412.
40. Feng, D.; Caulfield, D. F.; Sanadi, A. R. *Polym. Comp.* **2001**, *22*, 506.
41. Xu, Z. H.; Niu, Y. H.; Yang, L.; Xie, W. Y.; Li, H.; Gan, Z. H.; Wang, Z. G., *Polymer* **2010**, *51*, 730.
42. Yasuniwa, M.; Tsubakihara, S.; Sugimoto, Y.; Nakafuku, C. *J. Polym. Sci. Pol. Phys.* **2004**, *42*, 25.
43. Yu, L.; Petinakis, E.; Dean, K.; Liu, H. S.; Yuan, Q. A. *J. Appl. Polym. Sci.* **2011**, *119*, 2189.
44. Shin, B. Y.; Jang, S. H.; Kim, B. S. *Polym. Eng. Sci.* **2011**, *51*, 826.
45. Radjabian, M.; Kish, M. H.; Mohammadi, N. *J. Appl. Polym. Sci.* **2010**, *117*, 1516.
46. Fambri, l.; Migliaresi, C. In Poly(lactic acid): Synthesis, Structures, Properties, Processing, and Applications; Auras, R.; Lim, L.-T.; Selke, S. E. M.; Tsuji, H., Eds.; Wiley: New York, **2010**.
47. Saeidlou, S.; Huneault, M. A.; Li, H.; Park, C. B. *Progr. Polym. Sci.* **2012**, *37*, 1657.
48. Taguet, A.; Huneault, M. A.; Favis, B. D. *Polymer* **2009**, *50*, 5733.
49. Li, G.; Favis, B. D. *Macromol. Chem. Phys.* **2010**, *211*, 321.
50. Majumdar, B.; Paul, D. R., Eds. Reactive Compatibilization; Wiley: New York, **2000**.
51. Larocca, N. M.; Ito, E. N.; Rios, C. T.; Pessan, L. A.; Bretas, R. E. S.; Hage, E. *J. Polym. Sci. Pol. Phys.* **2010**, *48*, 2274.
52. Majumdar, B.; Paul, D. R.; Oshinski, A. *J. Polymer* **1997**, *38*, 1787.
53. Groeninckx, G.; Harrats, C.; Thomas, S., Eds. Reactive Blending with Immiscible Functional Polymers: Molecular, Morphological, and Interfacial Aspects; Hansers: Munich, **2001**.
54. Jerome, R.; Pagnoulle, C., Eds. Key Role of Structural Features of Compatibilizing Polymer Additives in Reactive Blending; Hansers: Munich, **2001**.
55. Park, C. D.; Jo, W. H.; Lee, M. S. *Polymer* **1996**, *37*, 3055.